EFDA–JET–CP(14)01/15

H.G. Esser, V. Philipps, M. Freisinger, A. Widdowson, K. Heinola, A. Kirschner,
S. Möller, P. Petersson, P. Wienhold, S. Brezinsek, A. Huber, G.F. Matthews,
M. Rubel, G. Sergienko and JET EFDA contributors

Material Deposition on Inner Divertor Quartz Microbalance Systems during ITER–Like Wall Operation in JET

Material Deposition on Inner Divertor Quartz Microbalance Systems during ITER–Like Wall Operation in JET

H.G. Esser[1], V. Philipps[1], M. Freisinger[1], A. Widdowson[2], K. Heinola[3], A. Kirschner[1], S. Möller, P. Petersson[4], P. Wienhold[1], S. Brezinsek[1], A. Huber[1], G.F. Matthews[2], M. Rubel[4], G. Sergienko[1] and JET EFDA contributors*

JET-EFDA, Culham Science Centre, OX14 3DB, Abingdon, UK

[1]Institute of Energy and Climate Research, Forschungszentrum Jülich, Trilateral Euregio Cluster, D-52425 Jülich, Germany
[2]EURATOM-CCFE Fusion Association, Culham Science Centre, OX14 3DB, Abingdon, OXON, UK
[3]TEKES, University of Helsinki, P.O. Box 64, 00560 Helsinki, Finland
[4]Royal Institute of Technology,VR, SE-100 44 Stockholm, Sweden
** See annex of F. Romanelli et al, "Overview of JET Results", (24th IAEA Fusion Energy Conference, San Diego, USA (2012)).*

Preprint of Paper to be submitted for publication in Proceedings of the 21st International Conference on Plasma Surface Interactions, Kanazawa, Japan 26th May 2014 - 30th May 2014

ABSTRACT

The migration of beryllium, tungsten and carbon to remote areas of the inner JET-ILW divertor and the accompanying co-deposition of deuterium has been investigated using post-mortem analysis of the housings of quartz-micro balances (QMBs) and their quartz crystals. The analysis of the deposition provides that the rate of beryllium atoms is significantly reduced compared to the analogue deposition rate of carbon during the carbon wall conditions (JET-C) at the same locations of the QMBs. A reduction factor of 50 was found at the entrance gap to the cryo-pumps while it was 14 under tile 5, the semi-horizontal target plate. The deposits consist of C/Be atomic ratios of typically 0.1-0.5 showing an enrichment of carbon in remote areas compared to directly exposed areas with less carbon. The deuterium retention fraction D/Be is between 0.3 and 1 at these unheated locations in the divertor.

1. INTRODUCTION AND MOTIVATION

The inner wall of JET cladded entirely with carbon-fiber composites (JET-C) did not meet the challenges for reactor relevant fusion devices. Neither lifetime of the CFCs due to erosion nor fuel accumulation due to co-deposition in remote areas was acceptable. Thus, JET was transformed in 2009 into a full metallic device with beryllium in the main chamber and tungsten in the divertor (JET-ILW) to mimic the ITER first wall and investigate it's plasma compatibility and predicted reduction in fuel retention [1]. Quartz-Micro-Balance systems (QMBs), already in operation in JET-C [2, 3], were employed to characterize material deposition and fuel retention in the sub-divertor region.. They were renewed before JET-ILW for comparison. In JET-C the majority of eroded material was deposited on remote divertor areas containing high amounts of fuel [4] measured by post-mortem-analysis, QMBs and other diagnostics. The plasma configuration was identified as key parameter determining net carbon deposition/erosion on the QMB crystals. Strike-point locations closest to the QMBs revealed highest deposition strongly influenced by plasma conditions of preceding discharges. Carbon migrates stepwise by plasma induced re-erosion from plasma-wetted to shadowed areas. Deposition was largest when QMB-crystal and strike point was line-of sight, confirmed by optical spectroscopy [5] and. ERO modelling [6]. This paper reports solely on post-mortem analysis of outer QMB heat shields (Q-OHS) and deposition quartzes (Q-DEPO) during JET-ILW.

2. EXPERIMENTAL CONDITIONS

After the first ILW operation campaigns (Pulse No's: 80170–83794) QMBs were removed. The results presented originate from the analysis of 2 QMBs (QMB3 and QMB4) both located on the inner divertor module 2 in octant 1 (Fig.1).

2.1. QMB3 AND QMB4; LOCATIONS AND EXPOSURE CONDITIONS

QMB3 was fixed to a carbon-rib of the inner wide carrier, behind tile 3 (Fig.1). The lower end of the outer-heat-shield (Q3-OHS) with the aperture for the deposition quartz (Q3-DEPO) which is recessed by 1.3cm protrudes ≈ 28mm into the entrance slot of the pump duct. It has a direct line-of-sight to

horizontal tile 4. A shutter allows exposure of Q3-DEPO and partly of Q3-OHS during dedicated plasma phases. Three zones of different deposition thickness were formed depending on open/ close times of the shutter (Fig.2). Zone-I, including Q3-DEPO, was solely exposed during shutter open. Zone-II, (largest deposition), was always exposed independent of shutter position and Zone-III was always exposed except when the shutter was open. The deposit of Zone I solely originates from two JET-operation phases. Phase-1 after start of operation (Pulse No's: 80170–80333) and phase-2 at the end of the campaign before the QMBs were removed (Pulse No's: 83649–83794). The contribution from phase-1 is small and can be neglected, since only ohmic plasmas with ion fluxes as low as $1\times10^{21}[D^+/s]$ were executed during that phase / / resulting in D^+-fluencies smaller than 10% of phase-2 [5]. QMB4 was positioned beneath tile5 (Fig.1). A pyramid-shaped aperture within the protection tile provides an opening towards the inner divertor. It's not tungsten coated on the inner sides and may therefore act as secondary C source. The QMB crystal Q4-DEPO , recessed by 1.1 cm behind an aperture in Q4-OHS, and partly Q4-OHS are in line-of-sight with the vertical tile 3. Q4-OHS is recessed by 4.5cm from the front surface of the protection tile. QMB4 has no shutter, thus belongs to flux type zone-I, always exposed. The exposure conditions for the different zones with corresponding D^+-fluencies into the inner divertor measured by Langmuir probes are listed in table/1/.

2.2 POST-MORTEM ANALYSIS METHODS

Several methods were used to quantify areal densities of Be, W, C and D of the deposits. Nuclear-reaction analysis (NRA) was applied using a 1mm ^{3}He beam of 2.95MeV. to detect Be (^{9}Be(^{3}He,p)11B), to detect C, (^{12}C(^{3}He,p)^{14}N), and to detect D (D(^{3}He,p)^{4}He). W was quantified by Rutherford backscattering (RBS). In addition Be,C and W was measured with Electron Microprobe analysis (EPMA) based on emission of characteristic X-rays from a volumes of a few μm^3. Secondary ion mass spectrometry (SIMS) has been used to measure depth profiles of the elements and to quantify it's thickness at the craters by stylus profilometry. D retained in the layer was quantified by Laser-induced desorption combined with quadrupole mass spectrometry (LID-QMS) A 3ms laser pulse (beam width of ≈2–3mm) heats a local spot of the deposit to temperatures > 1000°C, desorbing hydrogen isotopes into a calibrated volume with subsequent quantification by quadrupole mass spectroscopy [8].

3 .EXPERIMENTAL RESULTS

Particle fluxes directed towards the QMBs, local geometry conditions and the shadowing of different QMB areas by the shutter lead to strong inhomogeneous deposits in poloidal and toroidal direction as shown by the interference colours in figures 2 and 4. This was already observed previously during JET-C [9]. Figures 3 and 5 show exemplarily areal densities of Be, C, W and the retained D. EPMA measurements were made along line scans oriented poloidal for Q3-OHS and toroidal for Q4-OHS (Q4-OHS is tilted by 90° compared to Q3-OHS). Further analysis methods were applied near these line scans, see spots in figures 2 and 4, according to the description in chapter 2.2.

3.1 OUTER HEAT SHIELD OF QMB3 (Q3-OHS)

The line scan on Q3-OHS crosses all particle fluence zones described above. The most striking result is the small amount of deposition (Be + C + W), showing a maximum of ≈ 10^{18}(Be+C+W)/ cm^2. This corresponds to a maximum layer thickness of ≈ 360nm assuming a layer density of ≈0.5 g/cm^3, deduced from areal density and layer thickness. Considering e.g. zone-III, exposed for most of the operation time (see table 1), a large variation of Be, C and W deposition along the poloidal direction was measured, for Be from about 1.3×10^{17} to 7×10^{17} Be/cm^2 and for W from 5×10^{15} to 4.5×10^{16} W/cm^2, respectively. Around y = 35mm a laser spot is crossed thus no EPMA data are shown. Note, NRA analysis spots are shifted toroidally with respect to the EPMA line scan. Thus measured values are slightly influenced by decreasing deposition in toroidal direction. The transition from zone-III to zone-II, exposed all the time, is hardly seen, since the exposure time increases by only 6%. At y = 25mm zone-I is reached showing a drop in deposition >10, zone-II was only exposed in phase-1 and phase-2 of the JET operation with solely identical H-Mode shots in phase-2. In general, EPMA, NRA and LID-QMS data agree satisfactory. The C/Be ratio of these deposits varies between 0.2-0.5 C/Be and the D/(Be+C+W)ratio on both heat-shields is near unity, but were found lower on Q3-DEPO and Q4-DEPO with values of D/Be ≈ 0.3 probably caused by larger temperature excursions. The W ratio (W/Be+C) of the thicker deposits (zone II, III, y>25mm) ranges from 0.05 to 0.1. The thin deposits in zone-I (y<25mm), created mainly during phase-2, are only ≈10nm, clearly measurable by EPMA, NRA and LID The larger C fraction in that zone is probably influenced by the C-background originating from surface and bulk contamination of the SS substrate. LID-QMS and NRA agree well, showing an areal density of ≈ 1×10^{16} D/cm^2. The W deposition is well above the detection limit of RBS and EPMA.

3.2 OUTER HEAT SHIELD OF QMB4 (Q4-OHS)

Q4-OHS see fig4 located under tile 5 see fig1 shows Be-amounts comparable to zone-II on Q3-OHS. Its maximum is about 6×10^{17} Be/cm^2 whereas the C-fraction is somewhat lower with values of ≈0.12-0.15 C/Be. The C deposition for y>40mm is again influenced by the C-background. The W/Be-ratio decreases from thickest toward thinner deposit from 0,05 to 0,01 and the D-retention D/(Be+W+C) behaves similar. The thin deposits on Q4-OHS are located on areas shadowed from direct view to tile 3. 16 different SIMS analyses performed as well on thick as on thin deposits on both Q-OHS showing homogenous depth profiles of Be and C. A decrease of the C content from interface to surface was not observed despite decreasing C in the plasma with operation time was observed by spectroscopy/ / and was found in deposits on other locations [11]. Local C-sources could be as well the reason for this phenomenon. Both quartz crystals of the QMBs have been analysed on one spot by NRA. Carbon was not measurable due to the overlap of NRA signals from the gold interlayer at the interface and the SiO2 substrate. The Be deposition on Q3-DEPO is 4.7×10^{16} Be/ cm^2. It's very thin and comparable to zone-I on Q3-OHS.. On Q4-DEPO the Be-deposition is as well comparable with that on the nearby Q4-OHS and amounts to about ≈ 8×10^{17} Be/cm^2.

4. DISCUSSION

The most important result is the low overall material deposition on the JET-ILW QMBs compared with previous JET-C campaigns. The maximum deposition on zone-II of Q3-OHS amounts to 1×10^{18} (Be+C+W) atoms/cm^2. The areal density of Be on zone-I was 2-3 $\times10^{16}$ Be/cm^2 and on Q3-DEPO 4.7×10^{16} Be/cm^2 corresponding to an averaged Be deposition rate of 2.8×10^{13} Be/cm^{2}s. During JET-C the C-deposition on the housing of the QMB3 was not analysed in detail, but estimated to >10μm. However, the analysis of the quartz showed a thickness of 1850nm, formed during 1.8 h time of exposure corresponding to a C-deposition rate of 1.3×10^{15}C/cm^{2}s and an atom deposition ratio of C(JET-C)/Be(ILW) of ≈50. This simple comparison does not consider the influence of the plasma configuration and other parameters. However, there is only little deposit on the sloping part of tile 4 which could have been re-eroded. Tile 4 would represent the primarily deposition zone for the same configurations in JET-C. Nevertheless strike point resolved analysis of C-deposition on the inner QMB shows [12] that the above derived overall deposition (1.3×10^{15} C/cm^{2}s) is a good representative value for H-mode plasmas. The measured deposition rate of 2.6×10^{13} Be/cm^{2}s for Q4-DEPO can directly be compared with those under C walls with the strike point positions on tile 3 for which a deposition rate of 3.9×10^{14} C/cm^{2}s was derived. Thus, a reduced deposition ratio of Be(ILW)/C(JET-C) of 4.2 (campaign-averaged) or 16 (considering only tile 3 strike point positions for JET-C was found. A strong reduction in material deposition with JET-ILW was also observed in other post-mortem analysis on tile surfaces [13] or rotating mirrors [11]. Furthermore most of the deposition in the divertor under JET-ILW is confined on top of the inner divertor baffle (apron tile 1), where the SOL plasma hits the wall, while the deposition strongly decreases along the vertical target on tile 1 and 3, showing finally rather thin deposits (≈1μm) on the horizontal tile 4. This shows a largely reduced transport of material along the vertical targets down into the divertor towards tile 4, which is in line with the low deposition rates measured here at the QMB locations. The reduced transport of particles is due to reduced erosion of the metallic Be compared to the C-erosion in JET-C Furthermore, while the Be and C are at first place deposited onto the apron of tile 1, Be has a reduced re-erosion by sputtering due to the low plasma temperatures in the inner divertor, whereas carbon atoms are chemically eroded and transported further even at the lowest plasma temperatures. This behaviour can be followed directly by the Be and C composition of the deposits, showing an increasing C fraction of the deposits when moving down along the inner targets [14]. Obviously, the residual carbon in ILW undergoes still the stepwise transport by chemical erosion, leading to an C-enrichment of the deposits on remote areas. This is in line with the material composition on the QMBs measured here showing quite small ratios of C/Be of 0.2–0.5 for Q3-OHS and 0.05-0.15 for Q4-OHS respectively. This C fraction is much larger than the C fraction in the ILW plasmas of less than 0.1% [10]. In all deposits W could clearly be measured with fractions of 0.02–0.1 W/(Be+C). This is large compared with that found typically inside the plasma, where the relative W/Be is typically <0.01. It indicates that the W found in the deposits is mainly produced by local sources on the inner W-targets near the QMBs. Thus, not all the local inner divertor W-sources are suppressed by Be. The data show also, that the W/Be fraction in deposits

decreases in areas shadowed from the plasma. This indicates that transport by multiple reflection is stronger for Be than for W. A large retention fraction of D/(Be+C+W) has been found in the deposits, approaching almost unity on the outer heat shields. A similar large D retention on remote deposits has been already reported in [13]. This fraction is large compared to the one observed in pure Be deposits [15], in particular for the low flux and impact energy conditions, which must be assumed for the present conditions. While the D retention fraction is large, the absolute amount of D retained in the layers at these remote areas is low due to the small overall deposition on these areas. The reduction of the overall D retention observed by gas balance measurements [16] results mainly from the reduced Be erosion during the X point operation, when compared with that of carbon. It is also promoted by the reduced transport of Be from the plasma-wetted to shadowed areas leading to reduced formation of D-rich deposits on these locations.

CONCLUSION

The analysis of the deposits on the QMB systems in the inner divertor show that the migration of Be to remote areas in JET-ILW is strongly reduced compared to C migration in JET-C. This is due to a reduced Be-source in the main chamber during X point operation and small re-erosion probability of deposited Be on the inner target tiles due to low plasma temperatures in the inner divertor. On the contrary carbon atoms migrate by re-erosion promoted by chemical erosion even at the lowest plasma temperatures. Also under ILW conditions, with C as a minority impurity, the residual carbon still migrates towards these areas, leading to enrichment of C in these layers. The absolute amount of deuterium retained in the remote areas is low even if the D-retention, i.e. the ratio of D/(Be+C+W), is approaching unity. This is due to the reduced amount of Be-erosion, total material migration and codeposition with fuel. The D retention ratio in these deposits is high (0.2-1) which is higher compared with the retention predicted by the empirical scaling for pure Be layers [15].

ACKNOWLEDGEMENT

This project has received funding from the European Union's Horizon 2020 research and innovation programme under grant agreement number 633053. The views and opinions expressed herein do not necessarily reflect those of the European Commission

REFERENCES

[1]. V. Philipps et al, Fusion Engineering and Design **85** (2010) issue 7-9 p 1581.
[2]. H.G. Esser et al., Fusion Engineering and Design **66-68** (2003) 855-860
[3]. H.G. Esser et al, Physica Scripta **T111** (2004) 129-132.
[4]. Coad J.P. et al Physica Scripta **T145**(2011) 014003 (6pp)
[5]. S, Brezinsek et al. Journal of Nuclear Materials **438** (2013) p303
[6]. A. Kirschner et al,Journal of Nuclear Materials **337–339** (2005) 17–24
[7]. K. Krieger et al. Journal of Nuclear Materials **438** (2013) p262
[8]. M. Zlobinski et al., Fusion Engineering and Design **86** (2011) 1332–1335

[9]. H.G. Esser et al. Journal of Nuclear Materials **363–365** (2007) 146–151
[10]. S. Brezinsek et al 2013 Nuclear Fusion **53** 083023
[11]. J. Beal et al, this conference
[12]. H.G. Esser et al. Journal of Nuclear Materials **390–391** (2009) 148–151
[13]. A. Widdowson et al, Physica Scripta, **T159**, 2014
[14]. S. Brezinsek 25th IAEA conference, St. Petersburg, EX/ P5-26
[15]. G. De Temmerman, Nuclear Fusion **48** (2008) 075008
[16]. T. Loarer et al, Journal of Nuclear Materials **438** (2013) 108-S113.

Zones	exposure time	D^+ fluence into divertor
Zone I Q3-OHS Q3-DEPO	0,51 h	Total: $2{,}3\times10^{26}$ Phase I: 1.1×10^{25} Phase II: 2.2×10^{26}
Zone II Q3_OHS Q4-OHS Q4- DEPO,	13,08 h	2,03E+27
Zone III QMB 3	12,34	1,79E+27

Table1: Exposure times and integrated ion fluxes measured by Langmuir probes for the different exposure zones of the QMBs.

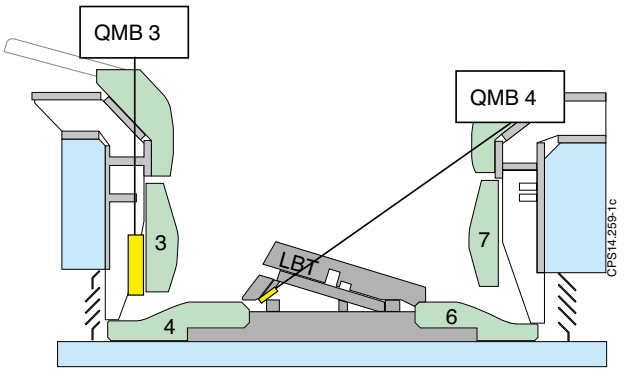

Figure 1: Location of QMBs in the JET divertor.

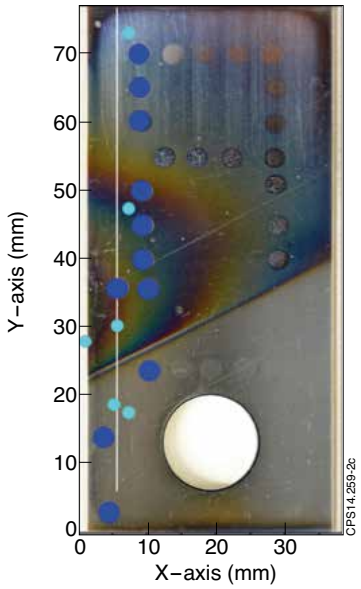

Figure 2: View of the outer heat shield Q3-OHS after exposure. Analysis of line and spots shown in figure 3.

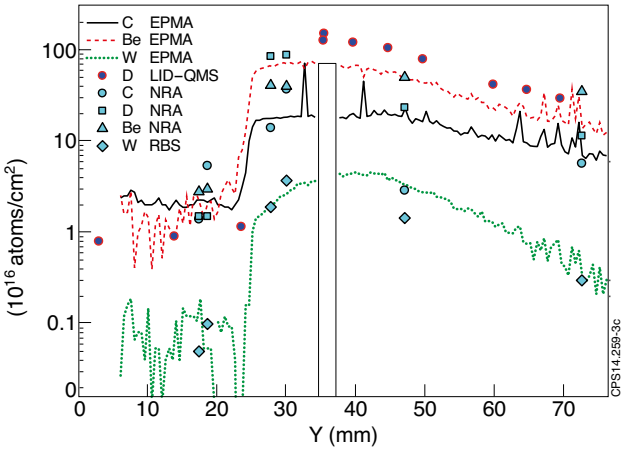

Figure 3: Be, C, W and D areal density measured by various analysis methods as marked in figure 2.

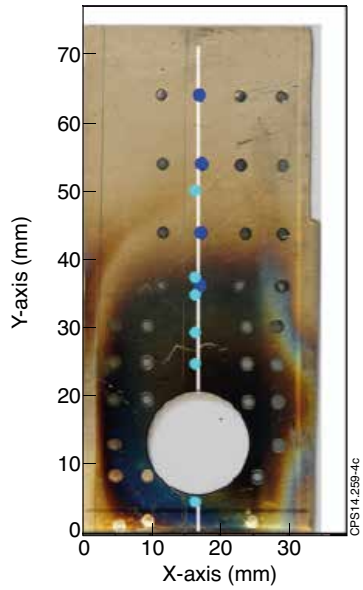

Figure 4: View of the outer heat shield Q3-OHS after exposure. analysis of line and spots shown in figure 3.

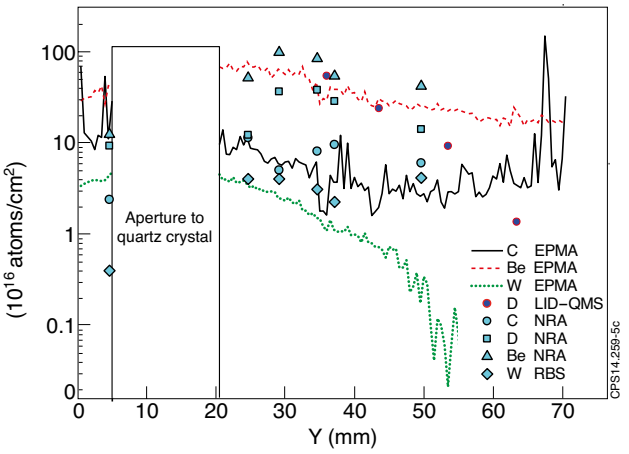

Figure 5: Be, C, W and D areal density measured by various analysis methods as marked in figure 4.